JOURNAL OF VIROLOGY, Oct. 1996, p. 6723–6732 Vol. 70, No. 10
0022-538X/96/$04.00+0


# Role of the DIS Hairpin in Replication of Human Immunodeficiency Virus Type 1

BEN BERKHOUT* AND JEROEN L. B. VAN WAMEL

*Department of Human Retrovirology, Academic Medical Center, University of Amsterdam, Amsterdam, The Netherlands*

Received 3 April 1996/Accepted 7 June 1996

**The virion-associated genome of human immunodeficiency virus type 1 consists of a noncovalently linked dimer of two identical, unspliced RNA molecules. A hairpin structure within the untranslated leader transcript is postulated to play a role in RNA dimerization through base pairing of the autocomplementary loop sequences. This hairpin motif with the palindromic loop sequence is referred to as the dimer initiation site (DIS), and the type of interaction is termed loop-loop kissing. Detailed phylogenetic analysis of the DIS motifs in different human and simian immunodeficiency viruses revealed conservation of the hairpin structure with a 6-mer palindrome in the loop, despite considerable sequence divergence. This finding supports the loop-loop kissing mechanism. To test this possibility, proviral genomes with mutations in the DIS palindrome were constructed. The appearance of infectious virus upon transfection into SupT1 T cells was delayed for the DIS mutants compared with that obtained by transfection of the wild-type provirus (pLAI), confirming that this RNA motif plays an important role in virus replication. Surprisingly, the RNA genome extracted from mutant virions was found to be fully dimeric and to have a normal thermal stability. These results indicate that the DIS motif is not essential for human immunodeficiency virus type 1 RNA dimerization and suggest that DIS base pairing does not contribute to the stability of the mature RNA dimer. Instead, we measured a reduction in the amount of viral RNA encapsidated in the mutant virions, suggesting a role of the DIS motif in RNA packaging. This result correlates with the idea that the processes of RNA dimerization and packaging are intrinsically linked, and we propose that DIS pairing is a prerequisite for RNA packaging.**

The genomes of retroviruses consist of two identical full-length RNA transcripts that are linked by noncovalent bonds (50). The nature of this RNA-RNA interaction is unknown. Electron microscopic studies showed an apparent parallel interaction near the 5′ ends of the two RNA molecules in a region called the dimer linkage structure (DLS). Dimerization is generally believed to play an important role in the preferential encapsidation of viral genomes within the budding virus particle and in the process of reverse transcription. For instance, a dimeric genome allows the viral reverse transcriptase (RT) enzyme to bypass occasional breaks in one of the RNA genomes (23), and the presence of a diploid genome was suggested to enhance genetic recombination, which may increase the rate of retroviral evolution (22, 39, 46, 50). Because the sequences located between the major splice donor (SD) (Fig. 1) and the *gag* gene are present in full-length genomic RNA but absent from all spliced mRNA forms, this region of the leader has received the greatest attention as the determinant for RNA dimerization and packaging (50).

Several molecular mechanisms of retroviral genome dimerization have recently been proposed on the basis of in vitro studies with relatively short RNA fragments (2, 6, 10, 12, 13, 15, 29, 32, 38, 43, 45, 47). Some reports described an important role for the viral nucleocapsid protein NCp7 in the formation of RNA dimers (13, 15), an effect that is probably related to the ability of NC protein to activate base pair rearrangements (49). However, spontaneous RNA dimerization is possible in the absence of any viral or cellular protein, and protein is not required to hold the two RNA molecules together because genomic RNA can be phenol extracted from mature virion particles as a dimer.

Several attempts have been made to map the region responsible for dimerization of the RNA genome of human immunodeficiency virus (HIV). A 100-nucleotide RNA fragment located downstream of the major SD site was initially reported to dimerize efficiently, and "purine quartets" were proposed to trigger dimerization within this part of the HIV type 1 (HIV-1) leader RNA (2, 32, 47). This DLS interaction, which is schematically depicted as model A in Fig. 1, is based on the presence of several consensus PuGGAPuA tracts in the DLS region downstream of the SD site. An analogous mechanism has been proposed previously for dimerization of telomeric DNA through formation of quadruple helical structures that are stabilized by guanine base tetrads (9). The HIV-2 leader RNA, for instance, encodes 4 such motifs ($_{271}$GGGAAA$_{276}$, $_{284}$AGGAAA$_{289}$, $_{447}$AGGAGA$_{452}$, and $_{541}$GGGAGA$_{546}$), with an additional motif in the 5′ end of the *gag* open reading frame ($_{573}$GGGAAA$_{578}$). Nevertheless, we reported efficient dimerization of mutant HIV-2 leader transcripts that were deleted for all purine motifs (7), and virion-extracted HIV-1 RNA dimers were not stabilized by potassium, an effect expected for guanine quartets (18). Several studies with HIV-1 RNA mutants also reported the involvement of sequences outside the original DLS region. In particular, a dimerization initiation site (DIS) upstream of the SD site was identified between nucleotides 250 and 272 of the HIV-1 genome (models B and C in Fig. 1). The rate of RNA dimerization was increased in the presence of this motif, although a lower thermal stability was measured for this DIS dimer than for the previously defined DLS dimer (29, 36, 38, 45).

The DIS motif consists of a palindromic sequence in the loop of a hairpin structure (Fig. 2). Dimerization has been proposed to initiate via loop-loop interaction solely on the

* Corresponding author. Mailing address: Department of Human Retrovirology, Academic Medical Center, University of Amsterdam, Meibergdreef 15, 1105 AZ Amsterdam, The Netherlands. Phone: (31-20) 5664822. Fax: (31-20) 6916531.

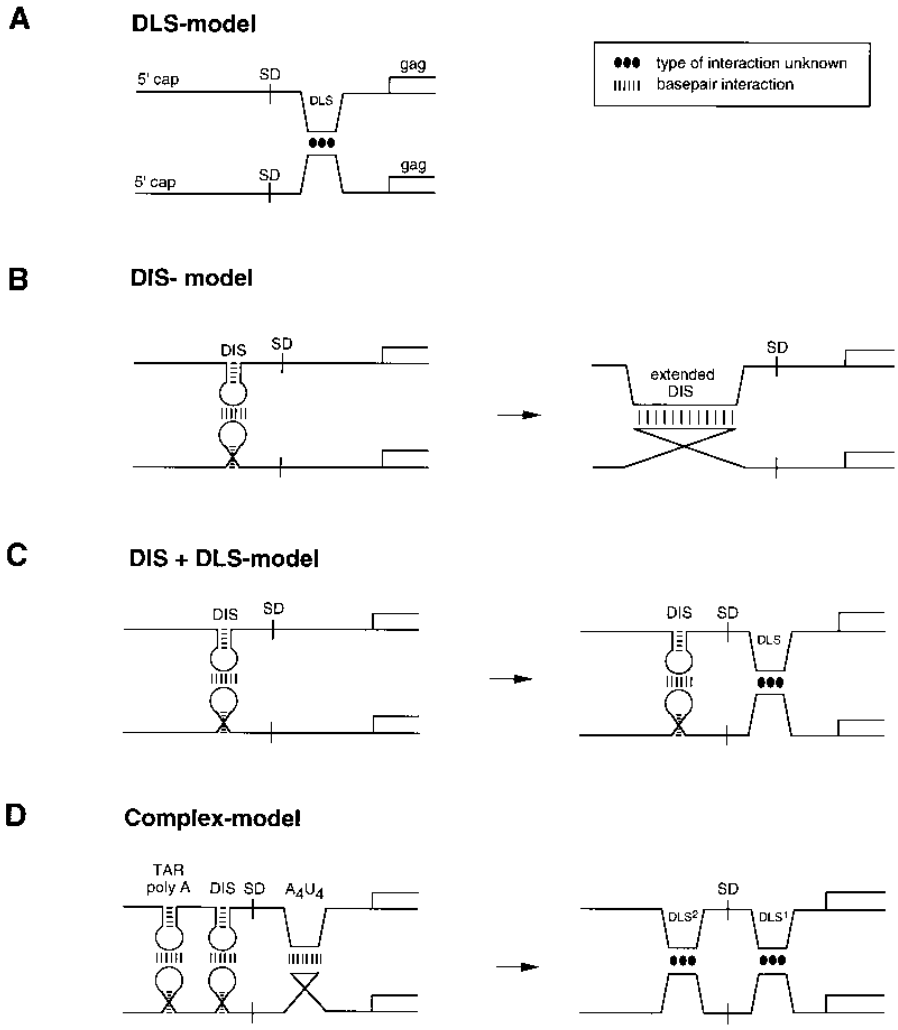


FIG. 1. Models for HIV-1 RNA dimerization and maturation. A schematic is shown of the HIV-1 leader RNA from 5′ cap to the start of the *gag* open reading frame. Model A is the classical DLS model, with an unknown type of RNA-RNA interaction downstream of the SD. Different kinds of RNA-RNA interactions could be involved in retroviral genome dimerization: either regular Watson-Crick base pairing (| | |; e.g., loop-loop kissing of DIS) or noncanonical base pairings in parallel or antiparallel configuration, tertiary RNA structures, or purine quartets (●●●). We do not know whether the two RNA strands interact in a parallel or antiparallel fashion. Although electron micrographs show parallel RNA strands, the resolution of these images is insufficient to rule out local antiparallel interactions through folding of the RNA molecule. The proposed DIS loop-loop kissing interaction (in models B to D) is shown as a crossed hairpin to highlight the antiparallel nature of this base pairing. Multistep RNA dimerization is presented in models B to D. Here, RNA dimerization is initiated through the DIS motif, and subsequent maturation-stabilization of the dimer occurs either through extended DIS-DIS interactions (model B) or through additional interactions in the downstream DLS region (model C). Model D differs from the previous models at several points: (i) motifs other than DIS are involved in the initial RNA dimer interaction [e.g., the palindromic loops of the upstream *trans*-acting responsive (TAR) and poly(A) hairpins or the $A_4U_4$ motif downstream of the SD site], (ii) the DIS dimer constitutes part of the packaging signal, and (iii) the DIS-DIS duplex is replaced in the mature dimer by DLS interactions of unknown nature. See the text for further details.

basis of Watson-Crick base pairing (29, 36, 38, 45). The palindromic character of the loop was demonstrated to be essential for in vitro dimerization. A number of single base changes in the palindrome (e.g., GUGCAC to GCGCAC or GUGCGC) completely abolished dimerization, but the double mutant with a repaired palindrome, GCGCGC, was fully active (38). Several models were proposed to explain maturation and further stabilization of the initial DIS dimer. Subsequent opening of the DIS stem may further stabilize the structure by the formation of additional intermolecular base pairs (model B in Fig. 1) (29, 36). Alternatively, the initial DIS dimer can mature through additional RNA interactions in the downstream DLS region (model C in Fig. 1) (33, 38, 45). Thus, although there is convincing evidence for a critical role of the DIS motif in in vitro dimerization, the nature of other sequence and/or structure motifs involved in this process remains largely obscure. Infection experiments with HIV-1 mutants were initiated in this study to further elaborate on the mechanism of retroviral RNA dimerization.

## MATERIALS AND METHODS

**HIV-1 plasmids.** The infectious HIV-1 molecular clone pLAI (a generous gift of Keith Peden [41]) was used to construct the two DIS mutants used throughout this study. The unique *Bss*HII site, corresponding to the $_{257}$GCGCGC$_{262}$ (GC3) palindromic loop sequence of the DIS hairpin, was cleaved and treated either with S1 nuclease or Klenow polymerase in the presence of deoxynucleoside triphosphates (dNTPs) according to standard procedures (44). The DNA was transfected into *Escherichia coli* after ligation of the blunt ends. The mutations within the DIS loop were verified by sequence analysis. The resulting plasmids are termed GC1 and GC5, with GC3 being the parental HIV-1 LAI molecular clone. The GC5 mutant was described previously in studies on the mechanism of cleavage site recognition by restriction endonuclease *Bss*HII (8).

**Tissue culture, DNA transfection, and virus infection.** The SupT1 T-cell line was grown in RPMI 1640 medium containing 10% fetal calf serum (FCS) at 37°C

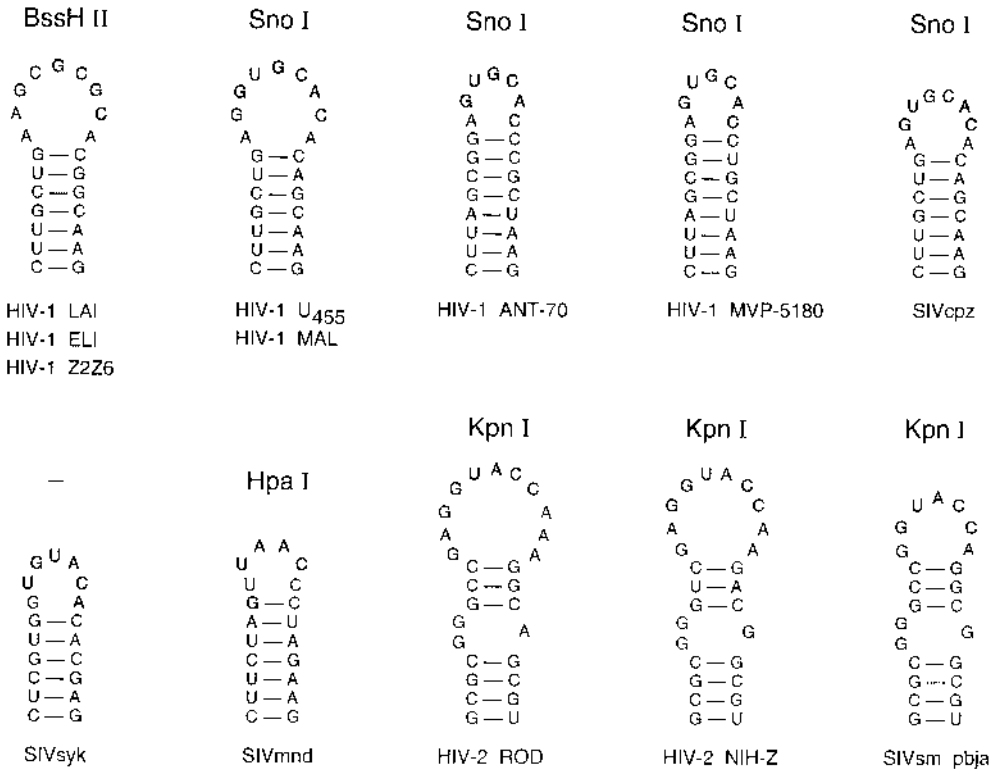


FIG. 2. Phylogenetic comparison of DIS RNA hairpin structures of different HIV and SIV strains. The primate lentiviruses analyzed include HIV-1 and HIV-2 and several SIV strains identified in a number of Old World monkey species: the sooty mangabey (SIVsm), mandrill (SIVmnd), African green monkey (SIVagm), Sykes monkey (SIVsyk), and chimpanzee (SIVcpz) (37). The palindromic motifs in the loop are marked by grey boxes, and restriction enzymes with the corresponding cleavage sites are listed above the hairpins. Although no similar structure could be folded for SIVagm isolates, SIVagm isolates usually have a duplicated *Xho*I motif (CUCGAG) and a single *Apa*I sequence (GGGCCC) in this domain of the leader transcript.

and 5% $CO_2$. SupT1 cells were split 1 to 10 every 4 days and transfected by means of electroporation. A total of $5 \times 10^6$ cells were washed in RPMI 1640 medium with 20% FCS, resuspended in 250 μl of the same medium, mixed with 1 to 5 μg of plasmid DNA in 0.4-cm cuvettes, electroporated at 250 V and 960 μF, and resuspended in RPMI 1640 medium with 10% FCS.

Cultures with the replication-impaired HIV-1 mutants were used to select for faster-replicating revertants. A sample of the infected culture was used to inoculate an uninfected SupT1 culture such that syncytia were apparent after approximately 1 week. We initially passaged 1 μl of the GC1 and GC5 cultures onto a fresh 5-ml SupT1 culture, but the sample size was gradually reduced at later time points (e.g., 0.1 μl for GC5 after 6 weeks of culture). Proviral DNA was isolated from the two cultures at day 67 to analyze the proviral DIS sequence.

**CA-p24 ELISA.** Culture supernatant was heat inactivated (30 min at 56°C) in the presence of 0.05% Empigen, and the CA-p24 concentration was determined by twin-site enzyme-linked immunosorbent assay (ELISA) with alkaline-conjugated anti-p24 monoclonal antibody EH12-A (34). Recombinant CA-p24, expressed in a baculovirus vector, was used as reference standard.

**RT enzyme assays.** The RT enzyme was released from HIV-1 virions by Nonidet P-40 treatment (0.5% final concentration) (3) and assayed for activity with the poly(rA)-oligo(dT) template-primer pair as described previously (53). Reaction mixtures contained 60 mM Tris (pH 7.8), 75 mM KCl, 5 mM $MgCl_2$, 0.1% Nonidet P-40, 1 mM EDTA, 5 μg of poly$(rA)_{7000}$ per ml, 0.16 μg of oligo$(dT)_{15}$ per ml, 4 mM dithiotheitol, and 50 μCi of [$^{32}$P]dTTP (3,000 Ci/mmol) per ml. Samples were incubated at 37°C; 10-μl aliquots were removed after 3 h and spotted onto DEAE ion-exchange paper (DE81; Whatman). The filter was washed three times in 5% $Na_2HPO_4$ to remove unincorporated nucleotides and dried after two 96% ethanol washes. The spots were visualized by autoradiography and quantitated on a PhosphorImager.

**Virus preparation and RNA isolation.** Virus particles were collected as described previously (18). In brief, 10-ml aliquots of SupT1 culture supernatants were harvested at the peak of infection, as indicated by the presence of giant syncytia. Cells were removed by low-speed centrifugation (10 min at 1,500 rpm). The supernatant was filtered through a 0.45-μm-pore-size filter, and virion particles were pelleted by centrifugation at 25,000 rpm for 30 min at 4°C in a Beckman SW27 rotor. A virus pellet resulting from 10 ml of culture medium was resuspended in 500 μl of lysis buffer (50 mM Tris [pH 7.4], 10 mM EDTA, 1% sodium dodecyl sulfate [SDS], 100 mM NaCl). A 5-μl sample was removed for CA-p24 ELISA and RT activity assays. The remainder was supplemented with 5 μl of tRNA (50 μg of *E. coli* tRNA [RNase free] per ml; Boehringer Mannheim) and 5 μl of proteinase K (50 μg/ml; Boehringer Mannheim). The resuspended pellets were incubated at 37°C for 30 min, extracted with an equal volume of phenol, and subjected to phase separation by centrifugation after addition of an equal volume of chloroform-isoamyl alcohol (24:1). This treatment was repeated, and the viral RNA was precipitated from the aqueous layer by addition of 2.5 volumes of 96% ethanol and 0.1 volume of 3 M sodium acetate (pH 5.2) (30 min at −20°C). The RNA was pelleted (10 min at 14,000 rpm at 4°C) and rinsed with 70% ethanol. The pellet was dried briefly, dissolved in 50 μl of TE (10 mM Tris [pH 7.5], 1 mM EDTA), aliquoted, and stored at −80°C.

**RNA melting experiments and nondenaturing Northern (RNA) blot analysis.** In melting experiments, 1 μl of RNA sample was mixed with 9 μl of TEN-SDS buffer (10 mM Tris [pH 7.5], 1 mM EDTA, 1% SDS, 100 mM NaCl) and incubated for 10 min at various temperatures. For gel analysis, 4 μl of sample buffer (15% Ficoll 400, 0.25% bromophenol blue) was added to the samples. The RNA was separated on nondenaturing 0.9% agarose gels in 1× Tris-borate-EDTA buffer. Electrophoresis was at 100 V for approximately 4 h. The gel was soaked in 3 volumes of 10% formaldehyde at 65°C for 30 min, and the RNA was electroblotted (Bio-Rad chamber) onto a positively charged membrane (microporous nylon 66; Boehringer Mannheim). The damp membrane was UV cross-linked at 120,000 J/cm$^2$ (Stratalinker) and then prehybridized for 4 h at 65°C in buffer A (3× SSC [1× SSC is 0.15 M NaCl plus 0.015 M sodium citrate], 0.1% SDS, 10× Denhardt's solution, 50 μg of salmon sperm DNA per ml). Hybridization with the denatured HIV probe was done for 16 h at 65°C in buffer B (6× SSC, 0.1% SDS, 10% dextran sulfate, 50 μg of salmon sperm DNA per ml). The $^{32}$P-labeled HIV-1 DNA probe was generated by random-primer labeling (Boehringer Mannheim) of a *Bst*XI fragment of the *gag* gene (pLAI positions 1628 to 2403). Filters were washed four times in buffer C (1× SSC, 1% SDS) for 15 min at 65°C. The blots were quantitated with a PhosphorImager (Molecular Dynamics).

**Primer extension analysis.** Primer extension analyses of the viral RNA genome with exogenously added oligonucleotides or the endogenous tRNA primer were performed as described previously (14), with minor modifications. The RT enzyme used is a recombinant glutathione *S*-transferase–RT fusion protein purified from *E. coli* (37a). The primers used in this study are schematically de-

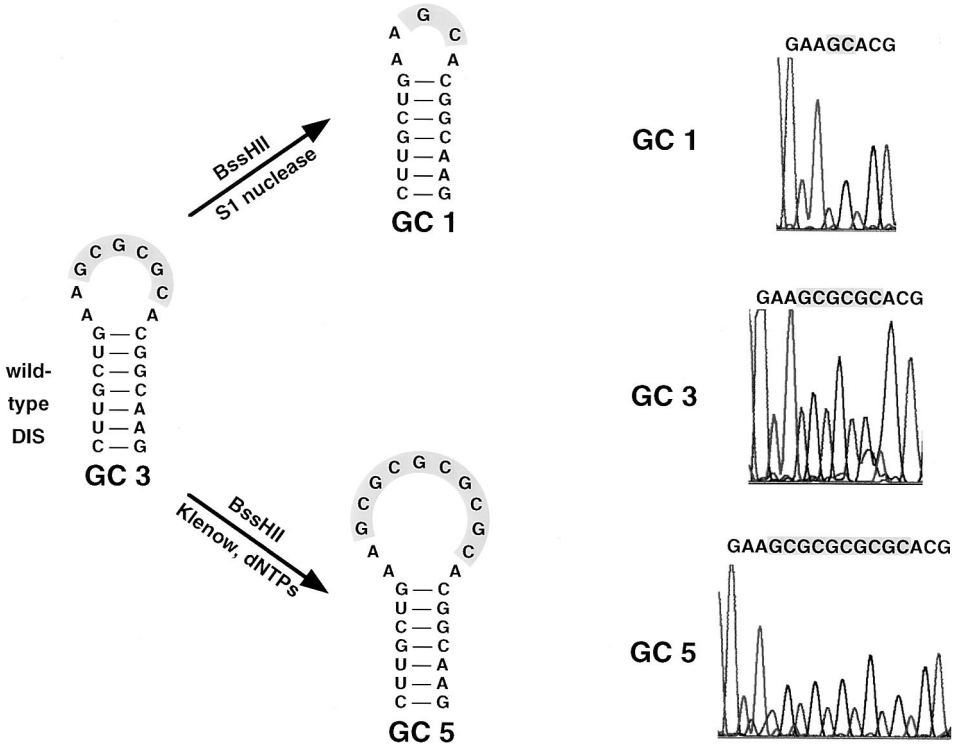


FIG. 3. Schematic of the DIS hairpin structure of mutants GC1 and GC5. The GC1 and GC5 mutants were generated by manipulation of the *Bss*HII restriction site encoded by the GC3 palindrome in the infectious plasmid pLAI. Details of the construction are described in Materials and Methods. The wild-type GC3 palindrome was either truncated to GC1 or extended to GC5 (grey boxes). Biochemical evidence for existence of the wild-type DIS hairpin was presented previously (21). The stem of the HIV-1 DIS region can be extended, with inclusion of internal loop and bulge elements, but not all HIV and SIV isolates can form an extended stem, and we therefore show only the top part of the hairpin. The RNA secondary structures presented for the GC1 and GC5 mutants were not probed experimentally. The GC3 (wild-type) and GC1 RNA structures are predicted by the MFold program, with calculated stabilities ($\Delta G$) of −7.4 and −8.3 kcal (1 cal = 4.184 J)/mol, respectively (shortening of the loop to five nucleotides as in GC1 marginally increases the stability of the hairpin). The MFold program predicts the GC5 hairpin, but with three additional G-C base pairs in the loop region formed between the first and last three nucleotides of the GC5 motif. This structure, with a four-nucleotide loop and an additional A-rich internal loop, has a predicted $\Delta G$ of −10.7 kcal/mol. The GC4 revertant obtained upon culture of the GC5 mutant (Fig. 9) has a deletion of one of these extra G-C base pairs, with a $\Delta G$ of −8.9 kcal/mol. Thus, both the GC5 mutant and GC4 revertant are not predicted to fully expose the GC palindrome in the single-stranded loop.

picted in Fig. 7. Gels were quantitated with a PhosphorImager (Molecular Dynamics).

**Proviral DNA analysis.** Proviral DNA was PCR amplified from total cellular DNA with primers 5′CE and SK39 as described previously (14). The PCR fragment was ligated into the TA cloning vector pCRII (Invitrogen) and sequenced with the universal T7 and SP6 primers and a *Taq* Dyeprimer cycle sequencing kit (Applied Biosystems) on an Applied Biosystems 370A DNA sequencer.

A radioactive DIS PCR was performed to detect nucleotide insertions or deletions in the DIS region of the mutant viruses upon prolonged culture. Proviral DNA was amplified with two primers flanking the DIS region: upstream (sense) primer PBS-18, corresponding to the primer binding site (PBS), and downstream (antisense) primer SD, which is complementary to the SD region (see Fig. 7). A 116-bp PCR fragment is generated on the wild-type pLAI sequence. After a standard PCR amplification of 35 cycles, 3 additional cycles were performed in the presence of [$\alpha$-$^{32}$P]dCTP. A 5-μl sample of the PCR mixture was mixed with 2.5 μl of formamide sample buffer, heated at 80°C, and analyzed on a denaturing 6% urea-polyacrylamide gel.

**RNA secondary structure analysis by computer folding.** RNA structure predictions and free energy calculations were performed with the MFold program in the University of Wisconsin Genetics Computer Group software package, version 7.2 (16). The MFold program (54) uses the energy rules as described by Freier et al. (17).

## RESULTS

**Phylogenetic conservation of a DIS hairpin with palindromic loop sequence.** We performed a phylogenetic analysis of the untranslated leader regions of the RNA genomes of several HIV and simian immunodeficiency virus (SIV) isolates. A structure similar to the DIS hairpin proposed for HIV-1 RNA could be folded for most virus isolates in similar regions of the leader transcript between the PBS and the major SD site (Fig. 2). The hallmark of the HIV-1 DIS motif is the 6-mer palindrome within the loop of a hairpin. These features are conserved among the different viruses, even though there is considerable sequence heterogeneity in both the stem and loop domains. In general, the base changes on one side of the DIS stem are compensated for by base substitutions in the opposite strand (base pair covariation). Remarkably, sequences in the loop also demonstrate covariation that maintains the palindromic character (palindromic covariation). For convenience, we listed the restriction endonucleases that recognize the different loop palindromes (Fig. 2; e.g., HIV-1 = GCGCGC = *Bss*HII and HIV-2 = GGUACC = *Kpn*I). Given the variety of palindromes used by the different viruses, it seems that the exact base sequence has relatively minor importance. Conservation of the palindromic character of six nucleotides in the DIS loop is fully consistent with the proposed Watson-Crick base-pairing function during HIV-1 RNA dimerization.

**Mutation of the DIS palindrome inhibits HIV-1 replication.** We constructed two mutant HIV-1 molecular clones with altered DIS loop sequences (Fig. 3). The wild-type GC3 palindrome of the LAI isolate was either truncated to GC or enlarged to GCGCGCGCGC in mutants GC1 and GC5, respectively. Although the extended palindrome in GC5 can theoretically form additional base pairs in a loop-loop kissing

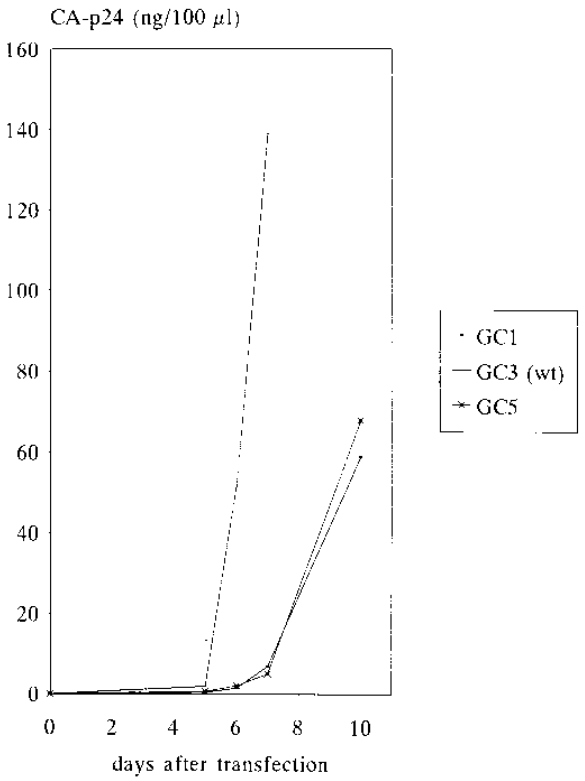


FIG. 4. Replication of wild-type and DIS-mutated HIV-1. SupT1 cells were transfected with 1 μg of the wild-type and DIS-mutated proviral constructs. Virus-associated CA-p24 production was measured in the culture supernatant at several time points.

complex, it is important to realize that the RNA secondary structure of this mutant may not be optimal for this type of interaction. For instance, three additional G-C base pairs can extend the DIS stem of this mutant such that the palindromic sequence is not fully exposed as single-stranded RNA (see the legend to Fig. 3). The wild-type and mutant HIV-1 plasmids were transfected into the SupT1 T-cell line, and virus spread was assayed by measurement of the virion-associated CA-p24 levels in the culture supernatant. We measured delayed replication kinetics for both mutants compared with wild-type HIV-1 (Fig. 4). In transfections with less plasmid DNA (<1 μg), we consistently did not observe virus production for either mutant after up to 3 weeks in culture, whereas the wild-type virus usually appeared in the second week (not shown). When more plasmid DNA (>5 μg) was used in the transfection, it was relatively easy to initiate a spreading infection leading to a fully infected culture, as evidenced by the presence of syncytia. This allowed us to obtain large amounts of virion particles for biochemical analysis of the genomic RNA. Thus, the GC1 and GC5 viruses demonstrate a replication defect, but both DIS mutants are not fully replication impaired.

**Dimeric RNA genomes are present in DIS-mutated HIV-1 virions.** The culture supernatant of SupT1 cells infected with wild-type or mutant HIV-1 was harvested at the peak of infection, as measured by CA-p24 levels and the appearance of giant syncytia. Virion particles were purified by centrifugation, and virion RNA was purified by phenol extraction. The RNAs were characterized by nondenaturing Northern analysis. Figure 5 shows that only one RNA species was present in the wild-type and mutant virions, suggesting that both mutants were able to assemble dimeric RNA genomes. To directly demonstrate that the observed RNA form corresponds to dimeric HIV-1 RNA, we incubated the samples at increasing temperatures before separation on the gel (Fig. 5). All three RNA samples converted into a faster-migrating form that corresponds to monomeric HIV-1 RNA. This result indicates that the DIS motif is not essential for formation of an RNA dimer, but the proposed loop-loop base pairing may contribute to the stability of the dimer. To test this, we accurately measured the thermal stability of the wild-type and mutants dimers by treating them in parallel at increasing temperatures in the range of 40 to 60°C (Fig. 6). All three RNAs were converted to the monomeric form at 60°C, with identical melting temperatures of 48°C.

Given the genetic instability of the mutant viruses (see below), it could be argued that the mutant virions used for RNA isolation do not correspond with the input mutant provirus. To prove that the GC1 and GC5 virions contain mutant RNA genomes with the four-nucleotide deletion and insertion, respectively, we performed primer extension assays. The C(N1) primer, complementary to a region of the HIV-1 RNA upstream of DIS (Fig. 7), produced identical cDNAs on the wild-type and mutant templates (Fig. 8, lanes 4 to 6). In contrast, priming from positions downstream of DIS (Fig. 7, primers SD and AUG) resulted in cDNAs differing in length (Fig. 8, primer SD in lanes 7 to 9 and primer AUG in lanes 10 to 12). These results clearly demonstrate the presence of mutant RNA genomes in the GC1 and GC5 viruses.

We also used the primers SD and AUG (Fig. 7) in an approach to probe for subtle differences in conformation of the wild-type and mutant RNA templates in the DIS dimerization region. This assay is based on the idea that dimer-specific RNA interactions in the leader transcript may abort reverse transcription initiated from a downstream position, resulting in the production of prematurely terminated cDNAs. The standard reverse transcription protocol cannot be used here because it includes an 82°C denaturation step that will melt the dimer

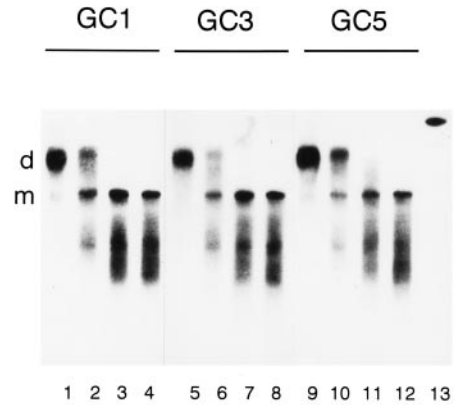


FIG. 5. Electrophoretic analysis of HIV-1 genomic RNAs from wild-type and mutant virions. Viral RNA was phenol extracted from purified virions and analyzed on a native 0.9% agarose gel. The GC1 mutant (lanes 1 to 4), GC3 wild type (lanes 5 to 8), and GC5 mutant (lanes 9 to 12) were heated for 10 min at increasing temperatures before analysis (45°C in lanes 1, 5, and 9; 50°C in lanes 2, 6, and 10; 55°C in lanes 3, 7, and 11; 60°C in lanes 4, 8, and 12). The RNA was electroblotted from the gel onto a membrane and visualized with a $^{32}$P-labeled HIV-1 probe. Positions of dimer (d) and monomer (m) RNA are indicated. Dissociation of the RNA dimer produces the monomeric form, but a smear of faster-migrating RNA species was consistently observed (e.g., lane 3). These smaller products were detected previously in studies with HIV-1 (18) and MoMLV (19) RNA genomes. We believe that this smear represents nicked RNA genomes that are part of the RNA dimer complex before denaturation. Plasmid pLAI was included in lane 13 as a reference sample.

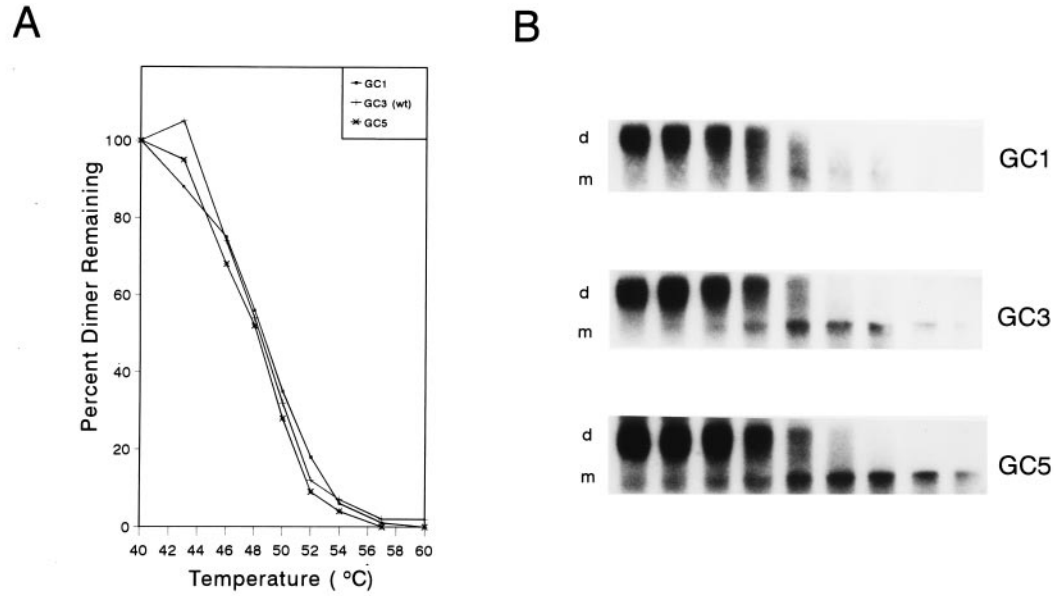


FIG. 6. Analysis of the thermal stabilities of wild-type and mutant RNA dimers. Aliquots of the virion-extracted RNA in TEN-SDS buffer were heated in parallel for 10 min at increasing temperatures (40, 43, 46, 48, 50, 52, 54, 57, and 60°C) and then analyzed on a native agarose gel (B). Positions of dimer (d) and monomer (m) RNA are indicated. The dimer bands were quantitated with a PhosphorImager, and the amount of dimer present at 40°C was set at 100% for each RNA sample (A).

(Fig. 6). Hence, annealing of the oligonucleotide primer on the dimeric RNA genome was performed at 20°C. As a control sample, the monomeric RNA was generated by preincubation of the sample at 60°C. Gel analysis of the cDNA products did not reveal any specific reverse transcription stops with the dimer templates compared with the corresponding monomers (results not shown). Apparently, the elongating RT enzyme can efficiently melt the putative dimer structure within the HIV-1 leader RNA, which is perhaps not surprising because RT has to proceed through this leader region in natural infections. More importantly, we did not detect any difference in cDNA production on the wild-type and mutant dimer templates (not shown). In conclusion, we measured efficient RNA dimerization and similar melting properties for the GC1 and GC5 mutants compared with the wild-type GC3 RNA.

**DIS mutants exhibit an RNA-packaging defect.** The processes of RNA dimerization and packaging may be linked both in time and place, that is, during virus assembly at the cell surface, and it was recently suggested that RNA dimerization is a prerequisite for subsequent packaging (18, 19). We therefore decided to accurately measure the RNA levels in the wild-type and mutant virus particles. The amounts of genomic RNA in the purified virion samples were analyzed by Northern blotting (Fig. 6B), and the efficiency of RNA packaging was calculated on the basis of the CA-p24 protein level as a virion marker (Table 1). A partial RNA-packaging defect was apparent for both mutants, consistent with the observed replication defect. As in all work involving DNA transfection and in vitro cell culturing, some experimental variation is expected from these assays. To assess whether the relatively minor variations in RNA levels reflect actual differences in RNA encapsidation, additional parameters were examined. RT activity was included as second, independent marker for the number of virions analyzed. Furthermore, we used primer extension assays as an additional RNA quantitation method (Fig. 8). The results (Table 1) demonstrate an approximately twofold reduction in RNA encapsidation efficiency for both DIS mutants. Thus, the

TABLE 1. Characteristics of genomic RNA in wild-type and mutant viral particles[a]

| Virus | RNA packaging efficiency (%) | | | | | |
|---|---|---|---|---|---|---|
| | RNA/CA-p24 | | | RNA/RT | | |
| | Northern[b] | C(N1)[c] | tRNA extension[d] | Northern | C(N1) | tRNA extension |
| GC3 (wt) | 100 | 100 | 100 | 100 | 100 | 100 |
| GC1 | 74 | 43 | 35 | 71 | 41 | 34 |
| GC5 | 56 | 41 | 51 | 52 | 38 | 47 |

[a] For all viruses tested, more than 95% of the genomic RNA was in the dimeric form, with a melting temperature of 48 ± 2°C.
[b] RNA measured by native Northern blot (arbitrary PhosphorImager counts [$10^4$]); average of three lanes (dimer band only) of the gel shown in Fig. 6B.
[c] RNA levels as determined in the C(N1) primer extension assays (e.g., Fig. 8).
[d] Viral RNA was quantitated in the tRNA extension assay (e.g., Fig. 8).

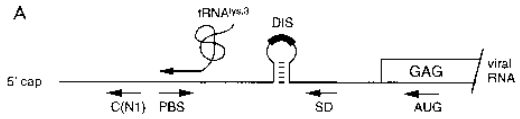


B

| | Primer extension | | | | DIS-PCR |
|---|---|---|---|---|---|
| | C(N1) | tRNA3Lys | SD | AUG | PBS + SD |
| GC1 | 151 | 257 | 293 | 370 | 112 |
| GC3 (wt) | 151 | 257 | 297 | 374 | 116 |
| GC5 | 151 | 257 | 301 | 378 | 120 |

FIG. 7. Primer extension assays and the DIS PCR strategy. (A) Schematic of the HIV-1 leader and part of the *gag* open reading frame. Indicated are the PBS and the associated $tRNA_3^{Lys}$ molecule, the DIS hairpin, and the positions of several antisense oligonucleotide primers used in reverse transcription (Fig. 8). Primers PBS-18 (sense) and SD (antisense) were used in the DIS PCR protocol (Fig. 9). (B) Lengths of the cDNA products (in nucleotides) for the different primer-template combinations. The lengths of the PCR reaction products (in base pairs) on the wild-type and mutant templates are also provided.

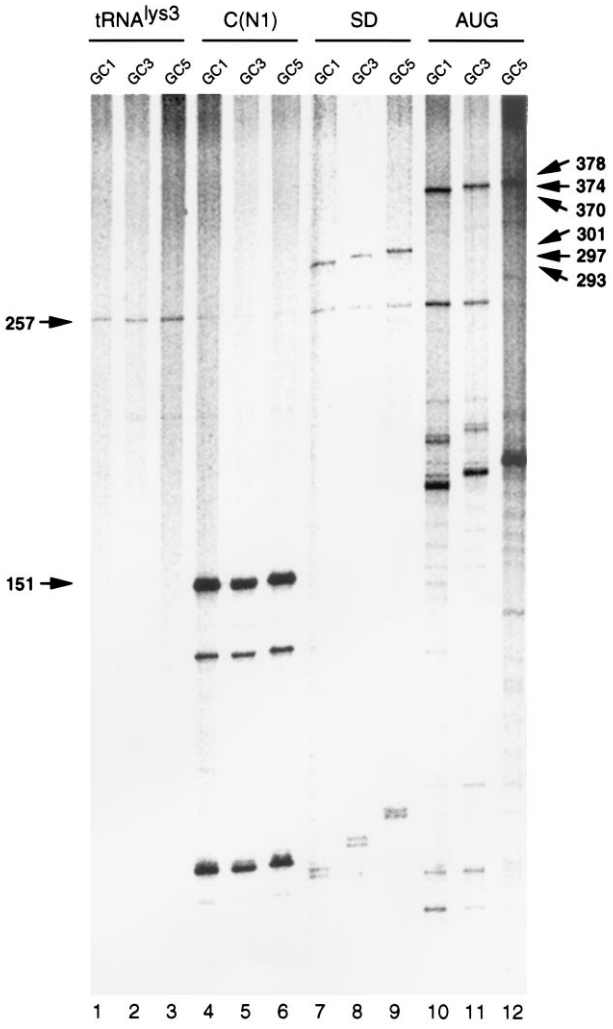


FIG. 8. Primer extension assays with wild-type and DIS-mutated RNA extracted from virions. The viral RNA was analyzed in oligonucleotide primer extension assays with primers complementary to different regions of the leader transcript (Fig. 7). The natural $tRNA_3^{Lys}$ primer, which remains associated with the viral RNA upon purification, was extended by the addition of RT and dNTPs. This 76-nucleotide tRNA primer produces a 257-nucleotide cDNA molecule. Products were analyzed on a 6% polyacrylamide sequencing gel.

mutant RNAs are packaged inefficiently, but the RNA molecules present in virion particles are exclusively in a dimeric conformation that is indistinguishable from that of a wild-type dimeric genome.

The results obtained so far indicate a subtle RNA-packaging defect for the DIS mutants, but other effects cannot be excluded. The DIS structure is located within the untranslated leader region of the HIV-1 genome that is loaded with regulatory sequences that control essential steps in viral replication (e.g., signals for transcription [*trans*-acting responsive hairpin], RNA processing [major SD], mRNA translation, and reverse transcription [PBS]). Thus, an adverse effect on any of these processes remains a possibility. Virus production was measured by transient transfection of CD4-negative (nonpermissive) cells that preclude a spreading infection. We transfected HeLa cells with the wild-type and mutant HIV-1 plasmids and assayed viral protein expression by Western blot (immunoblot) analysis of total cell extracts. No significant differences in the proviral expression levels were measured (not shown). Furthermore, we measured equal levels of virus production in the culture supernatant in CA-p24 ELISA and RT activity assays (data not shown). These results demonstrate that mutation of the DIS palindrome within the HIV-1 leader does not interfere with proviral expression and virus production.

Mutation of the DIS motif could affect the process of reverse transcription, which is initiated from a $tRNA_3^{Lys}$ primer bound to the upstream PBS (Fig. 7A). In particular, several reports proposed additional contacts between the tRNA primer and the viral RNA (1, 7, 24, 25, 52). Mutation of the DIS can potentially inhibit the processes of tRNA binding and/or extension, and this was tested with the virion-derived RNA genomes to which the tRNA primer remains associated upon RNA extraction. The tRNA-priming capacity can be assayed in vitro by the addition of dNTPs and RT (14). This tRNA extension assay measures both the presence of tRNA primer and the ability of the viral RNA-tRNA complex to initiate reverse transcription. We performed tRNA extension assays with the wild-type and mutant HIV-1 RNAs isolated from virus particles (Fig. 8, lanes 1 to 3). These results indicate that the DIS mutations do not affect the mechanisms of tRNA binding and initiation of reverse transcription.

**Revertant analysis of the DIS mutants.** Because the replication and RNA-packaging defect of the DIS mutants is relatively minor, we wanted to obtain additional evidence for the loss of infectivity of these viruses. Titration of the transiently produced virus stocks revealed an approximately 10-fold reduction in infectivity of the GC1 and GC5 virions compared with the GC3 wild type. An analysis of revertant viruses can provide supplementary information on the severity and nature of a replication defect. To explore the possibility that revertants of the GC1 and GC5 mutants could arise following long-term passage, we selected for faster-growing variants. The two HIV-1 mutants were cultured for a prolonged period of time by passage of small aliquots of infected cultures, as indicated by the presence of syncytia, to fresh SupT1 cultures. Acceleration of viral replication was apparent in the GC5 culture around week 6. To identify changes that might compensate the DIS defect, total cellular DNA was isolated from infected cells at day 67 posttransfection, and PCR was performed to amplify the HIV-1 long terminal repeat leader region (see Materials and Methods). The PCR-amplified DNA was then cloned and sequenced. The complete leader regions of two independent GC5 clones were analyzed, and both were found to contain an altered DIS sequence with a GC4 palindrome. No other changes were present in the leader region, suggesting that the GC5-to-GC4 mutation is solely responsible for increased replication and eventual outgrowth of the GC4 variant.

To carefully assess the difference in replication potential of the GC5 mutant and the GC4 revertant, we performed a radioactive DIS PCR on the cellular DNA samples taken at different days after transfection of the GC5 mutant. The DIS PCR is performed with the primers PBS and SD, which flank the DIS motif (Fig. 7A). A 116-bp fragment is produced with the wild-type pLAI sequence as the template. Analysis of the small PCR fragment on a denaturing sequencing gel allows one to discriminate between GC4 and GC5 genomes, which produce 118- and 120-bp fragments, respectively. Figure 9A shows that the GC4 revertant was first observed at day 42, and the GC5 mutant was outgrown by this faster-replicating variant by day 63. On the basis of the rapid outgrowth of the GC4 revertant, we estimate that the fitness of this virus is at least 30% higher than that of the GC5 mutant (28).

No mutations were found in the DIS regions of three independent GC1 clones at day 67. The GC1 culture was also screened for putative nucleotide insertions, but such revertants

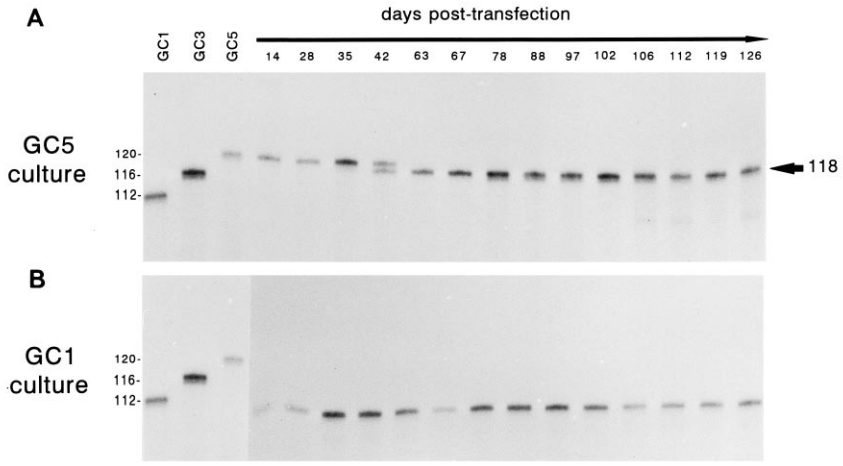


FIG. 9. Evolution of the DIS mutants in prolonged cultures. The SupT1 cell line was transfected with 5 μg of the GC1 and GC5 mutants. At the peak of infection, an aliquot of the culture supernatant was used to inoculate uninfected SupT1 cells. Cell samples were taken at several days posttransfection, and proviral DNA was amplified by the DIS PCR protocol (Fig. 7). The radiolabeled PCR products were analyzed on a sequencing gel (6% polyacrylamide-urea). Plasmids GC1, GC3 (wild type), and GC5 were used to generate size markers (112, 116, and 120 bp, respectively). Samples of the GC5 culture (A) and GC1 culture (B) were analyzed up to day 126 posttransfection. The 118-nucleotide fragment that appears in the GC5 culture around day 42 was demonstrated by sequence analysis to correspond to a GC4 revertant virus.

were not observed up to day 126 (Fig. 9B). Interestingly, sequencing of the day 126 sample revealed single-base substitutions in the DIS loop in all of the four clones analyzed. The A residue immediately downstream of the GC1 motif was found to be mutated to G. This point mutation partially restores the palindromic character of the DIS loop from GC1 to GC2, thus confirming the importance of this sequence motif in HIV-1 replication.

## DISCUSSION

The HIV-1 DIS element consists of an RNA hairpin structure with a 6-mer palindromic sequence in the single-stranded loop domain. On the basis of in vitro RNA dimerization studies, it is assumed that the DIS is functional as an RNA dimerization signal through base pairing of the autocomplementary loops on two identical RNA genomes (29, 36, 38, 45). We found the palindromic nature of the DIS loop to be conserved in most HIV and SIV isolates, despite considerable divergence in sequence of the loop palindrome. Furthermore, we observed a replication defect of HIV-1 constructs with a mutant DIS palindrome, arguing for an important role of this sequence in virus replication. Titration of transiently produced virus stocks revealed an approximately 10-fold reduction in titer (infectious units per CA-p24) of both DIS mutants compared with the wild-type virus. Surprisingly, the virions produced by the DIS mutants contained a dimeric RNA genome with a normal thermal stability. Mutation of the DIS palindrome did not affect *cis* elements of importance for proviral expression (transcription, mRNA transport, and translation) and virion production, but a small RNA-packaging defect was observed.

We measured a partial replication defect for the two DIS mutants, and a fully dimeric RNA genome could be extracted from the mutant virions, indicating that the DIS palindrome is not absolutely required for virus replication and RNA dimerization. This result differs significantly from results obtained in in vitro RNA dimerization studies. These studies unequivocally demonstrated that even single-base substitutions within the DIS palindrome abolish the ability to form RNA dimers (38). It is possible that HIV-1 replication kinetics measured in cell cultures understate the actual RNA dimerization/packaging defect. In vitro RNA dimerization studies clearly demonstrated that the RNA concentration is a critical parameter (6, 32), and it is possible that the number of RNA genomes per infected cell is particularly high in massively infected cell cultures because of the high multiplicity of infection. Under these conditions, a dimerization/packaging defect may be underscored. In other words, the minor packaging defect measured for the DIS mutants may be more pronounced in low-grade infections. This experimental problem seems hard to resolve because low-grade infections simply do not produce enough virus to perform biochemical RNA analyses. Another hypothetical explanation for the observation that the DIS is less critical in virus infection studies is that additional RNA elements are involved in RNA dimerization. We note that other leader regions both upstream and downstream of the DIS were demonstrated to trigger RNA dimerization in vitro (6, 32, 47), and some putative sites of dimerization are palindromes exposed in other single-stranded domains of the HIV-1 leader (4). For instance, the palindrome $_{77}$AAGCUU$_{82}$ in the loop of the upstream poly(A) hairpin (5) and the $_{302}$AAAAUUUU$_{309}$ octamer palindrome downstream of the SD site (43) may contribute to RNA dimerization through Watson-Crick base pairing (model D in Fig. 1). The idea of multiple RNA-RNA contacts is in agreement with previous observations by electron microscopy disclosing that retroviral RNA dimers are held together at many locations (31). Recently, Moloney murine leukemia virus (MoMLV) mutants lacking the DLS-psi region were found to produce virions with a high-molecular-weight RNA complex (48). These authors proposed that RNA linkage is not sequence specific but rather a result of special conditions encountered during particle formation, e.g., a high local RNA concentration.

We measured a small RNA-packaging defect for both DIS mutants. Consistent with this finding, a packaging defect has been reported previously for an HIV-1 variant with a mutation in the DIS region. A 13-nucleotide substitution affecting the 5′ half of the DIS hairpin resulted in a sixfold reduction in encapsidation of genomic RNA (26). A potential link between dimerization and encapsidation of retroviral genomic RNA has been proposed (18, 19). Studies with HIV-1 and other retro-

viruses suggest that their genomes are already joined into some dimeric structure at the time of virus assembly, consistent with the notion that a dimeric genome is specifically recognized during RNA encapsidation in assembling virions. Likewise, NC mutants of MoMLV contain very low levels of genomic RNA per virion, but these RNA genomes are almost exclusively dimeric (35). We hypothesize that RNA-protein contacts at the cell surface mediate the initial steps in RNA dimerization, e.g., DIS pairing, and that this RNA conformation is required for specific encapsidation. In other words, the requisite for packaging cannot be met by monomeric genomes (19). We propose that the DIS loop mutants demonstrate a partial dimerization defect that leads to inefficient RNA packaging. However, the fraction of the viral RNA that ends up in virion particles is fully dimeric. No absolute replication defect was scored for the DIS mutants, suggesting that additional RNA signals contribute to packaging. Indeed, although the leader region between the major SD and the *gag* gene has received the greatest attention (see the introduction), there is accumulating evidence that upstream leader sequences (20, 26, 51) as well as sequences within the 5′ part of the *gag* gene (11, 30, 40) contribute to the packaging function.

We analyzed revertant viruses to gain further insight into the nature of the DIS dimerization/packaging motif. The DIS loop of the GC1 deletion mutant acquired one base substitution after 126 days of culture. This mutation partially restored the palindromic nature from GC1 to GC2. The GC5 culture was overgrown by a GC4 revertant that first appeared at day 42. The GC5 to GC4 mutation is probably the result of slippage during reverse transcription of the GC-rich sequence. Upon copying of part of the GC motif, the nascent cDNA chain may dissociate and then reanneal to the wrong GC sequence. This type of mutation is frequently observed with retroviruses (27, 42). We had anticipated this slippage mechanism to generate the wild-type GC3 sequence as revertant in the prolonged GC5 culture. However, one should keep in mind that selection for revertant viruses is a chance process that depends on spontaneous mutations that occur early in the infected cell culture (27). We will continue to evaluate the GC4 culture for further improvement of virus replication. For instance, slippage-mediated deletion of another GC dinucleotide can produce the GC3 wild type, which may eventually happen if there is a substantial gain in fitness. Outgrowth of the GC4 variant is consistent with the idea that the GC5 palindrome is occluded by extended base pairing of the DIS stem (see the legend to Fig. 3).

Newly budded virions undergo a maturation process that alters the particle morphology. This maturation is induced by cleavage of the Gag and Gag-Pol polyproteins by the viral protease enzyme. The viral RNA genome also undergoes a maturation process. Although the RNA genomes of MoMLV and HIV-1 are already dimeric in rapid-harvest virus, the RNA increases its thermal stability and changes its electrophoretic mobility in native gels (18, 19). With protease-deficient mutants, it was demonstrated that RNA maturation depends on proteolytic cleavage of the viral polyproteins, and one of the cleavage products, e.g., the NC protein, may be involved in this process. We believe that the DIS interaction is resolved in the mature RNA dimer because the DIS palindrome did not contribute to the stability of the mature dimer (model D in Fig. 1). According to this RNA maturation mechanism, DIS loop-loop kissing occurs transiently only during the initial steps of RNA dimerization and packaging. Model D argues against RNA maturation through an extended DIS interaction through opening of the DIS stem as in model B. Dimer maturation and stabilization may involve unknown varieties of RNA interactions between undefined leader domains (schematically depicted in model D by $DLS^1$ and $DLS^2$). It is obvious that we cannot presently offer a more detailed model for retroviral RNA dimerization. We speculate that whereas in vitro dimerization studies highlight the initial DIS-like RNA contacts, the original electron microscopy studies revealed the mature DLS contacts.

In conclusion, this work lends credence to the idea that the processes of RNA dimerization and packaging are more intricately connected during the course of virion assembly than was previously thought. The RNA signals for both dimerization and packaging should be mapped in further detail, and it is anticipated that an intricate and subtle network of RNA-protein and RNA-RNA interactions are involved. It may turn out to be relatively difficult to dissect these molecular motifs because multiple, overlapping signals are involved. Although a combination of experimental approaches is therefore recommended, we particularly favor the analysis of HIV-1 revertants. A more extensive analysis may yield second-site revertants with mutations that can provide further insight into the RNA motifs involved. RNA structure probing of the genomes present in these virion particles may also help elucidate the molecular details of HIV-1 RNA dimerization and packaging.

## ACKNOWLEDGMENTS

We thank Atze T. Das for helpful discussions, Belinda Oude Essink for critical reading of the manuscript, and Wim van Est for artwork. We are grateful to Keith Peden for the pLAI molecular clone used in these studies.

This work was supported by the Dutch AIDS Foundation.

## REFERENCES

1. **Aiyar, A., D. Cobrinik, Z. Ge, H. J. Kung, and J. Leis.** 1992. Interaction between retroviral U5 RNA and the TYC loop of the tRNA(Trp) primer is required for efficient initiation of reverse transcription. J. Virol. **66:**2464–2472.
2. **Awang, G., and D. Sen.** 1993. Mode of dimerization of HIV-1 genomic RNA. Biochem. **32:**11453–11457.
3. **Back, N. K. T., M. Nijhuis, W. Keulen, C. A. B. Boucher, B. B. Oude Essink, A. B. P. van Kuilenburg, A. H. Van Gennip, and B. Berkhout.** 1996. Reduced replication of 3TC-resistant HIV-1 variants in primary cells due to a processivity defect of the reverse transcriptase enzyme. EMBO J. **15:**4040–4049.
4. **Berkhout, B.** 1996. Structure and function of the human immunodeficiency virus leader RNA. Progress Nucleic Acid Res. Mol. Biol. **54:**1–34.
5. **Berkhout, B., B. Klaver, and A. T. Das.** 1995. A conserved hairpin structure predicted for the poly(A) signal of human and simian immunodeficiency viruses. Virology **207:**276–281.
6. **Berkhout, B., B. B. Oude Essink, and I. Schoneveld.** 1993. In vitro dimerization of HIV-2 leader RNA in the absence of PuGGAPuA motifs. FASEB J. **7:**181–187.
7. **Berkhout, B., and I. Schoneveld.** 1993. Secondary structure of the HIV-2 leader RNA comprising the tRNA-primer binding site. Nucleic Acids Res. **21:**1171–1178.
8. **Berkhout, B., and J. L. B. van Wamel.** 1996. Accurate scanning of the BssHII endonuclease in search for its DNA cleavage site. J. Biol. Chem. **271:**1837–1840.
9. **Berkowitz, R. D., and S. P. Goff.** 1994. Analysis of binding elements in the human immunodeficiency virus type 1 genomic RNA and nucleocapsid protein. Virology **202:**233–246.
10. **Bieth, E., C. Gabus, and J.-L. Darlix.** 1990. A study of the dimer formation of Rous sarcoma virus RNA and its effect on viral protein synthesis in vitro. Nucleic Acids Res. **18:**119–127.
11. **Buchschacher, G. L., and A. T. Panganiban.** 1992. Human immunodeficiency virus vectors for inducible expression of foreign genes. J. Virol. **66:**2731–2739.
12. **Clever, J., C. Sassetti, and T. G. Parslow.** 1995. RNA secondary structure and binding sites for *gag* gene products in the 5′ packaging signal of human immunodeficiency virus type 1. J. Virol. **69:**2101–2109.
13. **Darlix, J.-L., C. Gabus, M. T. Nugeyre, F. Clavel, and F. Barre-Sinoussi.** 1990. Cis elements and trans-acting factors involved in the RNA dimerization of the human immunodeficiency virus HIV-1. J. Mol. Biol. **216:**689–699.
14. **Das, A. T., B. Klaver, and B. Berkhout.** 1995. Reduced replication of human immunodeficiency virus type 1 mutants that use reverse transcription primers other than the natural $tRNA_3^{Lys}$. J. Virol. **69:**3090–3097.

15. **De Rocquigny, H., C. Gabus, A. Vincent, M.-C. Fournie-Zaluski, B. Roques, and J.-L. Darlix.** 1992. Viral RNA annealing activities of human immunodeficiency virus type 1 nucleocapsid protein require only peptide domains outside the zinc fingers. Proc. Natl. Acad. Sci. USA **89:**6472–6476.
16. **Devereux, J., P. Haeberli, and O. Smithies.** 1984. A comprehensive set of sequence analysis programs for the VAX. Nucleic Acids Res. **12:**387–395.
17. **Freier, S. M., R. Kierzek, J. A. Jaeger, N. Sugimoto, M. H. Caruthers, T. Neilson, and D. H. Turner.** 1986. Improved free-energy parameters for predictions of RNA duplex stability. Proc. Natl. Acad. Sci. USA **83:**9373–9377.
18. **Fu, W., R. J. Gorelick, and A. Rein.** 1994. Characterization of human immunodeficiency virus type 1 dimeric RNA from wild-type and protease-defective virions. J. Virol. **68:**5013–5018.
19. **Fu, W., and A. Rein.** 1993. Maturation of dimeric viral RNA of Moloney murine leukemia virus. J. Virol. **67:**5443–5449.
20. **Geigenmuller, U., and M. L. Linial.** 1996. Specific binding of human immunodeficiency virus type 1 (HIV-1) Gag-derived proteins to a 5′ HIV-1 genomic RNA sequence. J. Virol. **70:**667–671.
21. **Harrison, G. P., and A. M. L. Lever.** 1992. The 5′ packaging signal and major splice donor region of human immunodeficiency virus type 1 have a conserved stable secondary structure. J. Virol. **66:**4144–4153.
22. **Hu, W.-S., and H. M. Temin.** 1990. Retroviral recombination and reverse transcription. Science **250:**1277–1233.
23. **Hu, W.-S., and H. M. Temin.** 1990. Genetic consequences of packaging two RNA genomes in one retroviral particle: pseudodiploidy and high rate of genetic recombination. Proc. Natl. Acad. Sci. USA **87:**1556–1560.
24. **Isel, C., C. Ehresmann, G. Keith, B. Ehresmann, and R. Marquet.** 1995. Initiation of reverse transcription of HIV-1: secondary structure of the HIV-1 RNA/tRNA(3Lys) (template/primer). J. Mol. Biol. **247:**236–250.
25. **Isel, C., R. Marquet, G. Keith, C. Ehresmann, and B. Ehresmann.** 1993. Modified nucleotides of tRNA(3Lys) modulate primer/template loop-loop interaction in the initiation complex of HIV-1 reverse transcription. J. Biol. Chem. **268:**25269–25272.
26. **Kim, H.-J., K. Lee, and J. J. O'Rear.** 1994. A short sequence upstream of the 5′ major splice site is important for encapsidation of HIV-1 genomic RNA. Virology **198:**336–340.
27. **Klaver, B., and B. Berkhout.** 1994. Evolution of a disrupted TAR RNA hairpin structure in the HIV-1 virus. EMBO J. **13:**2650–2659.
28. **Koken, S. E. C., J. L. B. van Wamel, J. L. M. C. Geelen, and B. Berkhout.** 1994. Functional analysis of the ACTGCTGA sequence motif in the human immunodeficiency virus type 1 long terminal repeat promoter. J. Biomed. Sci. **1:**83–92.
29. **Laughrea, M., and L. Jette.** 1994. A 19-nucleotide sequence upstream of the 5′ major splice donor is part of the dimerization domain of human immunodeficiency virus 1 genomic RNA. Biochemistry **33:**13464–13474.
30. **Luban, J., and S. P. Goff.** 1994. Mutational analysis of *cis*-acting packaging signals in human immunodeficiency type 1 RNA. J. Virol. **68:**3784–3793.
31. **Mangel, W. F., H. Delius, and P. H. Duesberg.** 1974. Structure and molecular weight of the 60–70S RNA and the 30–40S RNA of Rous sarcoma virus. Proc. Natl. Acad. Sci. USA **71:**4541–4545.
32. **Marquet, R., F. Baudin, C. Gabus, J. L. Darlix, M. Mougel, C. Ehresmann, and B. Ehresmann.** 1991. Dimerization of human immunodeficiency virus (type 1) RNA: stimulation by cations and possible mechanism. Nucleic Acids Res. **19:**2349–2357.
33. **Marquet, R., J. C. Paillart, E. Skripkin, C. Ehresmann, and B. Ehresmann.** 1994. Dimerization of human immunodeficiency virus type 1 RNA involves sequences located upstream of the splice donor site. Nucleic Acids Res. **22:**145–151.
34. **McKeating, J. A., A. McKnight, and J. P. Moore.** 1991. Differential loss of envelope glycoprotein gp120 from virions of human immunodeficiency virus type 1 isolates: effects on infectivity and neutralization. J. Virol. **65:**852–860.
35. **Meric, C., and S. P. Goff.** 1989. Characterization of Moloney murine leukemia virus mutants with single-amino-acid substitutions in the Cys-His box of the nucleocapsid protein. J. Virol. **63:**1558–1568.
36. **Muriaux, D., P.-M. Girard, B. Bonnet-Mathoniere, and J. Paoletti.** 1995. Dimerization of HIV-1 LAI RNA at low ionic strength. J. Biol. Chem. **270:**8209–8216.
37. **Myers, G., S. Wain-Hobson, L. E. Henderson, B. Korber, K. T. Jeang, and G. N. Pavlakis.** 1994. Human retroviruses and AIDS 1994. A compilation and analysis of nucleic acid and amino acid sequences. Theoretical Biology and Biophysics, Los Alamos National Laboratory, Los Alamos, N. Mex.

37a. **Oude Essink, B. B., et al.** Unpublished results.

38. **Paillart, J. C., R. Marquet, E. Skripkin, B. Ehresmann, and C. Ehresmann.** 1994. Mutational analysis of the bipartite dimer linkage structure of human immunodeficiency virus type 1 genomic RNA. J. Biol. Chem. **269:**27486–27493.
39. **Panganiban, A. T., and D. Fiore.** 1988. Ordered interstrand and intrastrand DNA transfer during reverse transcription. Science **241:**1064–1069.
40. **Parolin, C., T. Dorfman, G. Palu, H. Gottlinger, and J. Sodroski.** 1994. Analysis in human immunodeficiency virus type 1 vectors of *cis*-acting sequences that affect gene transfer into human lymphocytes. J. Virol. **68:**3888–3895.
41. **Peden, K., M. Emerman, and L. Montagnier.** 1991. Changes in growth properties on passage in tissue culture of viruses derived from infectious molecular clones of HIV-$1_{LAI}$, HIV-$1_{MAL}$, and HIV-$1_{ELI}$. Virology **185:**661–672.
42. **Pulsinelli, G. A., and H. M. Temin.** 1991. Characterization of large deletions occurring during a single round of retrovirus replication: novel deletion mechanism involving errors in strand transfer. J. Virol. **65:**4786–4797.
43. **Sakaguchi, K., N. Zambrano, E. T. Baldwin, B. A. Shapiro, J. W. Erickson, J. G. Omichinski, G. M. Clore, A. M. Gronenborn, and E. Appella.** 1993. Identification of a binding site for the human immunodeficiency virus type 1 nucleocapsid protein. Proc. Natl. Acad. Sci. USA **90:**5219–5223.
44. **Sambrook, J., E. F. Fritsch, and T. Maniatis.** 1989. Molecular cloning: a laboratory manual. Cold Spring Harbor Laboratory Press, Cold Spring Harbor, N.Y.
45. **Skripkin, E., J. C. Paillart, R. Marquet, B. Ehresmann, and C. Ehresmann.** 1994. Identification of the primary site of the human immunodeficiency virus type 1 RNA dimerization in vitro. Proc. Natl. Acad. Sci. USA **91:**4945–4949.
46. **Stuhlmann, H., and P. Berg.** 1992. Homologous recombination of copackaged retrovirus RNAs during reverse transcription. J. Virol. **66:**2378–2388.
47. **Sundquist, W. I., and S. Heaphy.** 1993. Evidence for interstrand quadruplex formation in the dimerization of human immunodeficiency virus 1 genomic RNA. Proc. Natl. Acad. Sci. USA **90:**3393–3397.
48. **Tchenio, T., and T. Heidmann.** 1995. The dimerization/packaging signal is dispensable for both the formation of high-molecular-weight RNA complexes within retroviral particles and the synthesis of proviruses of normal structure. J. Virol. **69:**1079–1084.
49. **Tsuchihashi, Z., and P. O. Brown.** 1994. DNA strand exchange and selective DNA annealing promoted by the human immunodeficiency virus type 1 nucleocapsid protein. J. Virol. **68:**5863–5870.
50. **Varmus, H., and R. Swanstrom.** 1991. Replication of retroviruses, p. 369–512. *In* R. Weiss, N. Teich, H. Varmus, and J. Coffin (ed.), RNA tumor viruses. Molecular biology of tumor viruses. Cold Spring Harbor Laboratory, Cold Spring Harbor, N.Y.
51. **Vicenzi, E., D. S. Dimitrov, A. Engelman, T.-S. Migone, D. F. J. Purcell, J. Leonard, G. Englund, and M. A. Martin.** 1994. An integration-defective U5 deletion mutant of human immunodeficiency virus type 1 reverts by eliminating additional long terminal repeat sequences. J. Virol. **68:**7879–7890.
52. **Wakefield, J. K., S.-M. Kang, and C. D. Morrow.** 1996. Construction of a type 1 human immunodeficiency virus that maintains a primer binding site complementary to $tRNA^{His}$. J. Virol. **70:**966–975.
53. **Willey, R. L., D. H. Smith, L. A. Lasky, T. S. Theodore, P. L. Earl, B. Moss, D. J. Capon, and M. A. Martin.** 1988. In vitro mutagenesis identifies a region within the envelope gene of the human immunodeficiency virus that is critical for infectivity. J. Virol. **62:**139–147.
54. **Zuker, M.** 1989. On finding all suboptimal foldings of an RNA molecule. Science **244:**48–52.